Cancer Immunology, Immunotherapy (2025) 74:343
https://doi.org/10.1007/s00262-025-04198-7

RESEARCH

Identification of two distinct uveal melanoma subtypes based on the immune cell infiltration of the primary tumour

Konstantinos Panagiotidis[1] · Sally Owens[2] · Grainne Finegan[1,2] · Noel Horgan[2] · Stefanos Tsavdaridis[3,4] · Susan Kennedy[2] · Achilleas Floudas[1,3]

Received: 1 September 2025 / Accepted: 7 October 2025

Abstract

Background Uveal melanoma (UM) is the most common intraocular malignancy, with poor prognosis in metastatic cases and limited response to conventional therapies. Despite advances in genetic stratification, the immunological landscape of primary UM remains poorly understood.

Methods Secondary data generation of single-cell RNA sequencing (scRNA-seq) of primary class 1 and class 2 (loss of *BAP1*) UM tumours and flow cytometric analysis of 8 primary UM tumour biopsies were used to characterize the tumour microenvironment, cellular composition, tumour–immune cell interactions, and stromal marker expression associated with tumour progression and immune infiltration.

Results scRNA-seq analysis revealed 16 distinct cell clusters, including melanocytes, T cells, macrophages, and stromal cells. Class 2 tumours contained unique melanocyte subpopulations exhibiting chromosome 8 copy number variations and enriched in hypoxia, PI3K-Akt, and MAPK signalling pathways. Ligand–receptor analysis identified extensive interactions between these aggressive melanocytes and pericytes/macrophages. Flow cytometric analysis confirmed two distinct immune infiltrate profiles: low-infiltrate tumours dominated by $CD14^+$ cells, and high-infiltrate tumours with $CD8^+$ memory-like T cells expressing PD-1 and CD27. Stromal marker analysis revealed elevated expression of CD81 and NGFR in immune-excluded tumours, implicating them in metastatic potential.

Conclusions Our study reveals cellular and immunological heterogeneity within primary UM tumours. The identification of immunologically distinct tumour types, along with aggressive melanocyte subpopulations and stromal interactions, provides insight into UM pathogenesis and supports stratified immunotherapeutic approaches.

Keywords Uveal melanoma · T cells · RNAseq · Lymphoid · Myeloid

Introduction

Uveal melanoma (UM) is the most common intraocular malignancy, accounting for approximately 3% of all melanoma cases [1]. Disease arises from melanocytes in the uvea tract of the eye with the majority of cases affecting the choroid and less frequently the iris and ciliary body. Mean patient age at diagnosis is 61 years, with fair-skinned people being at greater risk of developing UM [2, 3]. In Europe incidence shows a north-to-south gradient ranging from 2 cases per million in Italy to more than 8 in Denmark and Ireland [4, 5]. Treatment options aiming to achieve local tumour control include radiotherapy, transpupillary thermotherapy, and less often local resection; however for larger tumours enucleation may be required [6]. Despite the lack of detectable metastasis at the time of diagnosis, approximately half of UM patients develop secondary disease almost exclusively to the liver and more rarely to the skin, bone, and lung [7–9].

Almost all UMs harbour mutations in the Gq pathway with the majority involving GNAQ and GNA11. Despite

✉ Achilleas Floudas
achilleas.floudas@uoi.gr

1 School of Biotechnology, Dublin City University, Dublin, Ireland

2 Research Foundation, Royal Victoria Eye and Ear Hospital, Dublin, Ireland

3 Laboratory of Biology, Medical School, University of Ioannina, Ioannina, Greece

4 Department of Biological Applications & Technologyies,, University of Ioannina, Ioannina, Greece

their prevalence, these mutually exclusive mutations, are not sufficient to predict survival and are considered early drivers of the tumorigenic process prior to malignant transformation, which requires a second "hit" [10]. This event consists of an additional mutation, most commonly in the BAP-1 gene which is mutated in almost half of UM patients while SF3B1 and EIF1AX gene mutations are also frequent [11, 12]. Patients with loss of BRCA1-associated protein 1 (BAP-1) protein expression are in high risk of developing metastasis [13, 14]. BAP-1 is a tumour-suppressor gene, located on chromosome 3, that is commonly found mutated in mesothelioma and clear cell renal cell carcinoma in addition to UM. It encodes a nuclear deubiquitinase and is involved in a variety of cellular processes including DNA repair, cell cycle, survival and cell differentiation [15–17]. Patient cytogenetic characteristics and gene expression profiling (GEP) have been successfully utilized for stratifying patients with UM into different risk groups [18, 19]. Based on their GEP, UMs can be divided into 2 subgroups. Class 1 tumours show a lower metastatic potential and are generally characterized with normal chromosome 3 cytogenetics. On the contrary, class 2 UMs show significantly worse prognosis and are associated with concurrent mutations in BAP-1 and monosomy 3 leading to its bi-allelic loss [20]. Modern approaches utilizing multiplatform analysis have identified additional UM subsets. Patients with disomy 3 and mutations in EIF1AX and SF3B1 genes are characterized by good and intermediate prognosis, respectively, while patients with monosomy 3 are in greater risk for metastasis [21].

Despite the advancements in patient stratification, the survival rates of UM have not increased notably over the last decades, while some improvements are being attributed to earlier diagnosis [22–24]. Currently, there is no standard treatment for metastatic UM with patients responding poorly to chemotherapy [25]. Targeted therapies with inhibitors against recurrent mutations or overexpressed targets have been explored in clinical trials without succeeding in improving overall survival compared to chemotherapy [26, 27]. In contrast to cutaneous melanoma, immunotherapies such as immune checkpoint inhibitors (ICIs) show limited efficacy for treating UM patients, which is attributed to the lower mutational burden of UM and the immune privileged ocular microenvironment [28, 29]. Recently, Tebentafusp, a bispecific monoclonal antibody targeting CD3 and glycoprotein 100 [gp100], has been approved for the treatment of HLA-A*02:01–positive UM patients. Tebentafusp improved the 3-year overall survival of treatment naïve metastatic UM patients compared to ICI or chemotherapy monotherapies [30]. The encouraging results of Tebentafusp, despite the HLA restricted antigen presentation limitations, highlight the potential of immunomodulatory therapies for the treatment of UM and urge for deciphering its complex immune landscape.

In this study, we analysed the immune cell infiltrate from primary class 1 and class 2 UM tumours. We described the distinct cellular composition observed in the aggressive tumours and investigated putative interactions between immune and cancer cells that could drive disease progression. Additionally, we validated our findings by flow cytometric analysis of primary tumours. Our work suggests new potential insights into the complex tumoral microenvironment of UM.

Methods

Patient samples

Following written informed consent in line with the principles of the Declaration of Helsinki, eight primary tumour biopsies from treatment naive patients with UM treated with enucleation were obtained from the Royal Victoria Eye and Ear Hospital, Dublin, Ireland and ethical approval was obtained from the Ethics committee of the hospital, Ethics and Medical Research Committee of RVEEH. Enucleation specimens were delivered fresh to the pathology Department. Specimens were dissected and fresh tissue samples were collected and placed into a sterile container with RPMI (Lonza). The sample was then transported immediately to the Immunology Research Laboratory. Patient characteristics are listed in Table 1.

Flow cytometric analysis

Single cell suspensions of frozen primary UM tumour samples were generated by mechanical dissociation. Cells were stained with Zombie NIR fixable viability dye (Biolegend) and Fc receptor blocking was performed with Human TruStain FcX (Biolegend) prior to antibody staining. For the immune cell panel, expression of surface epitopes was investigated with the following fluorescently labelled antibodies: CD45-FITC (clone HI30) (Biolegend), CD3-APC (clone HIT3a)(Biolegend), CD4-Percp/Cy5.5 (clone OKT4)(Biolegend), CD8-BrilliantViolet785 (clone SK1)(Biolegend), CD56-BrilliantViolet421 (clone 5.1H11)(Biolegend), CD14-SparkBlue574 (clone HCD14)(Biolegend), CD206-PE/Fire700 (clone 15–2) (Biolegend), CD163-BrilliantViolet510 (clone GHI/61) (Biolegend), CD279-PE (clone NAT105)(Biolegend), CD27-BrilliantViolet605 (clone O323)(Biolegend), CD45RO-BrilliantViolet650 (clone UCHL1)(Biolegend). For the cancer cell panel, expression of surface epitopes was investigated with the following fluorescently labelled antibodies: CD45-BrilliantViolet421 (clone HI30)(Biolegend), CD271-PE/Cyanine7 (clone ME20.4)(Biolegend),

Table 1: Patient Demographics and Tumour Characteristic.

Total Cases	8	100%
Gender		
Male	5	**62.5%**
Female	3	**37.5%**
Age at operation		
Mean	63.63	
Median, (range)	61, (50–86)	
Enucleated eye		
Left	2	**25%**
Right	6	**75%**
Metastasis status		
No evidence of disease (NED)	8	**100%**
Alive with disease (AWD)	0	**0**
Dead of disease (DOD)	0	**0**
Dead of other causes (DOC)	0	**0**
Greatest tumour dimension (GTD) (mm)		
Mean	17.55	
Median, (range)	14.5 (5–43)	
Cell type		
Spindle	4	**50**
Epithelioid	1	**12.5**
Mixed	3	**37.5**
BAP1 IHC		
Expressed	2	**25**
Not expressed	6	**75**
FISH testing: monosomy 3		
Disomy 3	6	**75**
Monosomy 3	2	**25**
FISH testing: chromosome 8q gain		
Disomy 8	2	**25**
Chromosome 8q gain	6	**75**

NED no evidence of disease, *AWD* alive with disease, *DOD* dead of disease, *DOC* dead of other causes, *BAP1* BRCA1-associated protein 1, *BRCA1* breast cancer type 1 susceptibility protein, *IHC* immunohistochemistry, *FISH* Fluorescence in-situ hybridisation.

CD317-PerCP/Cyanine5.5 (clone RS38E)(Biolegend), CD55-BV510 (clone IA10)(BD), CD68-BrilliantViolet785 (clone Y1/82A)(Biolegend), CD81-BV605 (clone JS-81) (BD), CD276-BV650 (clone 7–517)(BD). Prior to staining of intracellular markers cells were fixed and permeabilized with the FOXP3 Fix/Perm Buffer Set (Biolegend). Intracellular staining was performed with the following fluorescently labelled antibodies: MART1-AlexaFluor594 (clone M2-7C10) (Biolegend), HMB45-AlexaFluor647 (clone HMB-45) (Biolegend), IRF7-AlexaFluor488 (clone 12G9A36) (Biolegend). Samples were acquired using a Cytoflex LX (Beckman Coulter) flow cytometer. Analysis was performed with FlowJo (v10) software. Flow cytometry data biplots were generated based on median fluorescence intensity values of samples stained and acquired on the same batch using packages ggbiplot, ggplot2 and ggfortify in R.

scRNA-seq analysis and data availability

The scRNA-seq uveal melanoma dataset GSE139829 was downloaded from the GEO database. Eight primary uveal samples were selected for downstream analysis. Empty droplets were excluded using the emptyDrops function of the DropletUtils R package (1.22.0) [31]. Seurat objects were generated using R package Seurat (5.1.0) and genes detected in less than 3 cells were excluded [32]. Elimination of doublets was performed using the DoubletFinder R package (2.0.4) [33]. Dead cells were filtered by excluding cells with more than 10% mitochondrial counts. Data normalization, which allows for mitigation of cell-to-cell variation due to technical factors, was performed using sctransform R package (0.4.1) [34]. In order to align cell populations from different datasets, they were integrated using the IntegrateData function of the Seurat package based on immune anchors with SCT as the normalisation method. Umap was generated by using the first 15 PCs and clustering was performed with findneighbours and findclusters functions of Seurat at a resolution of 0.5. Pathway enrichment analysis was performed under package PathfindR based on the Kyoto Encyclopedia of Genes and Genomes (KEGG). Receptor ligand interactions were generated with package nichenetr. A merged file from the previously described preprocessing steps, containing feature counts for each cell, as well as a gene position file and an annotation file were generated for input to inferCNV, no defined reference group was used.

Results

Single cell RNAseq analysis was performed on two class 1 (Bap1 wildtype) and six class 2 (BAP1 mutant) primary uveal melanoma tumours. Importantly, the analysis included only primary tumour cells and not cells from sites of metastasis. Following dead cell, multiplet exclusion and integration a total of 39,283 cells were maintained and clustered in 16 clusters. Seven clusters represent melanocytes, three T cells, three monocytes and macrophages, one photoreceptor cells, one pericytes and a smaller cluster of actively proliferating cells (Fig. 1A). The distribution of cells in the identified clusters per tumour sample is shown in Fig. 1B. At this resolution there is no cellular pattern to separate class 1 and class 2 UM tumour cellular landscape. However, specific samples show marked CD8 T cell infiltrate irrespective of class status (Fig. 1B). The identification of major infiltrating immune cell populations was based on expression of CD45

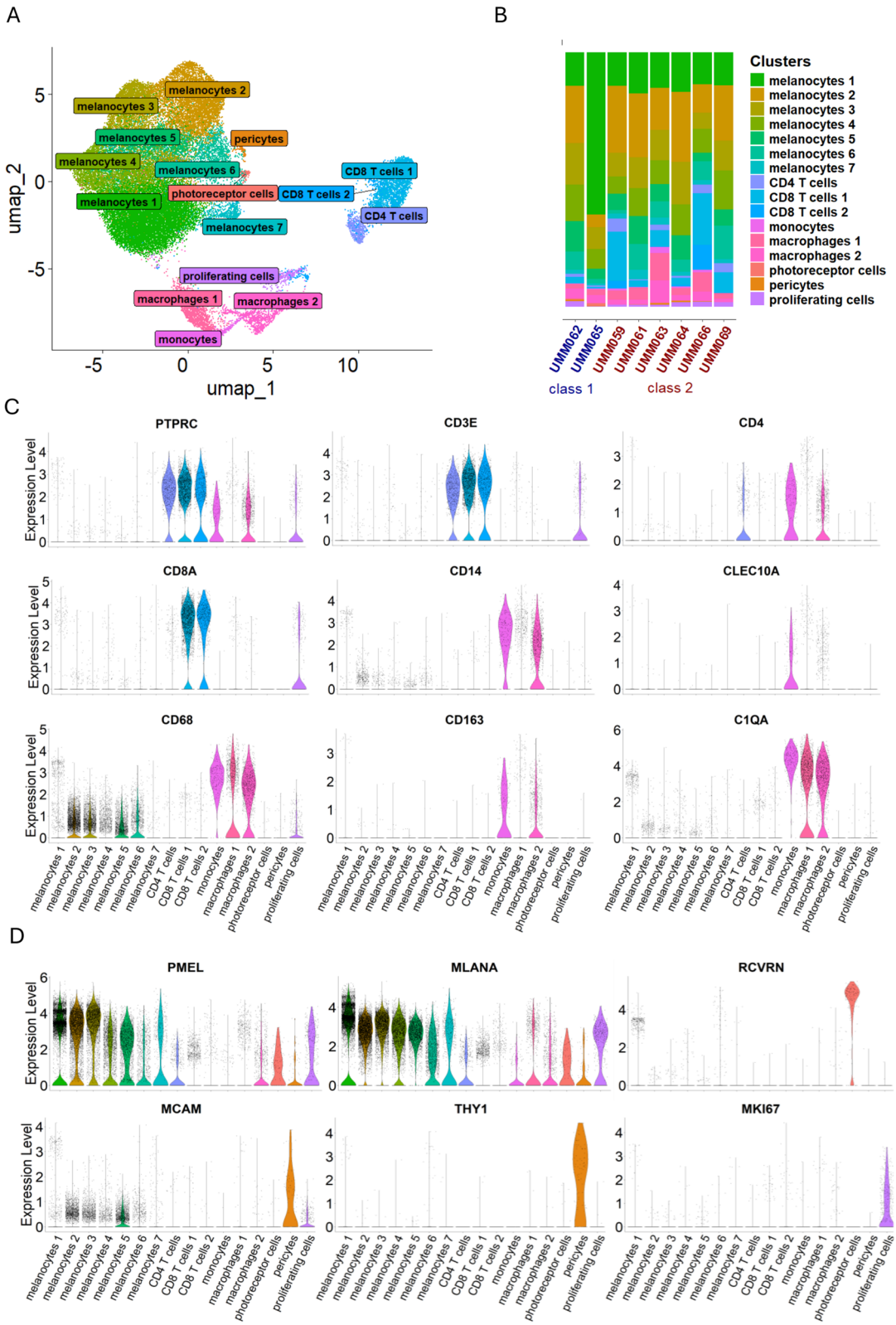

Fig. 1 Cellular landscape of class 1 and class 2 Uveal melanoma primary tumour. **A** UMAP of scRNAseq data from 2 class 1 and 6 class 2 UM primary tumours. **B** Distribution of the identified immune and stromal cell clusters per patient sample. **C** Violin plots depicting the expression of markers used for the annotation of immune cell populations. **D** Violin plots depicting the expression of stromal cell related markers used in cluster annotation.

(PTPRC) followed by interrogation of the expression of markers including CD3, CD4 and CD8 for the identification of T cell and, CD14, CD68, CLEC10A, C1QA, MARCO, CD163 for identification of monocytes and macrophages (Fig. 1C). Stromal and tumour cells were identified based on expression of PMEL and MLANA for melanocytes, MCAM for pericytes, RCVRN for photoreceptor cells and MKI67 for actively proliferating cells.

In order to assess differences in melanocyte populations between class 1 and class 2 primary UM tumours, the previously identified melanocyte clusters were subsetted, normalised and scaled followed by integration and clustering. A total of 12 melanocyte clusters from 31,312 cells were identified (Fig. 2A and B). Interestingly, clusters 3 and 6 are unique to the class 2 UM tumour biopsies. Following Copy Number Variation (CNV) analysis for the identification of genomic alterations that may contribute to cancer evolution clusters 2,3 and 6 showed marked copy number variations particularly for chromosome 8, which has been previously implicated in UM progression [35], # (Supplementary Fig. 1). Pathway enrichment analysis based on differentially expressed genes of cluster 3 and 6 compared to all other melanocyte clusters showed enrichment in hypoxia (HIF-1), metabolism (Oxidative Phosphorylation) and molecular signalling pathways (PI3K-Akt and MAPK) (Fig. 2 C and D). In order to assess potential interactions between cells belonging to cluster 3 and 6 and all other immune and stromal cells at the tumour site receptor ligand interaction analysis was performed. Differentially expressed receptors of melanocytes of cluster 3 and 6 (receiver cells) were identified and the expression of corresponding ligands by all other cells (sender cells) in the primary tumour site was analysed (Fig. 2E). Among the differential array of potential interactions between cluster 3 and 6 cells and immune and stromal cells at the primary tumour site, a high number of potential interactions with pericytes and macrophages were identified. (Fig. 2E).

Specific samples of the RNAseq dataset had marked T cell infiltration irrespective of BAP1 status. To further characterise the immune cell infiltrate flow cytometric analysis was performed on single cell suspensions of 8 primary uveal melanoma tumours, 2 of which had detectable BAP1 expression by IHC and 6 samples with loss of BAP1 and gain of 8q (Table 1). Following flow cytometric analysis with an immune cell specific antibody panel that included markers for most major T cell subsets and macrophages, comparable number of cells was selected by using function Downsample of FLowjo for each sample as to not bias the downstream analysis. The samples were then concatenated, and the dimensionality of the data was reduced by performing tSNE (Fig. 3A). Three major cell populations were identified, macrophages, T cells and NK cells (Fig. 3B and C). Similarly to the scRANseq analysis 2 distinct types of cell infiltrate were identified. Five primary tumour biopsies had a low overall immune cell infiltration and were characterised by increased percentage of CD14 + cells compared to CD3 + T cells (Fig. 3D). Three out of eight primary tumour biopsies harboured an immune cell infiltrate (CD45 +) that was dominated by CD3 + T cells ($^{*}p = 0.024$) the majority of infiltrating CD3 + T cells are CD8 + with high expression of memory associated marker CD27 and PD-1 (Fig. 3 D and F). In our cohort the CD3 high samples are PRAME + with an AJCC classification of T1-T4 while of the CD3 low, two are PRAME negative and 3 are PRAME positive with an AJCC classification of T2 and T3-T4 respectively.

In addition to the immune cell panel, paired flow cytometric analysis of stromal cells was performed. The biopsies were grouped into biopsies with a rich T cell infiltrate (CD3 +) or low T cell infiltrate (CD3-) based on the analysis of the immune cell panel (Fig. 4). Biopsies with low T cell infiltration show marked expression of CD81 which has been reported as a pro-metastatic factor of uveal melanoma exosomes and NGFR which is linked to invasiveness (Fig. 4). In order to assess whether alterations in the expression of stromal markers may be indicative of a disease specific pattern, PC analysis of flow cytometry derived mean fluorescent intensities (MFI) was performed. Interestingly, the three CD3 + UM biopsies show tight clustering compared to the more diverse clustering of CD3- UM biopsies (Fig. 4C).

Discussion

Uveal melanoma (UM) is known to not respond to immunotherapy in the same way as cutaneous melanoma and with the eye being an immunologically privileged site, studies on the immune cell environment are limited [36]. It is well established that UM is a heterogeneous disease with multiple classification systems, both clinical and genetic, in place to characterise the risk associated with disease aggressiveness and likelihood of progression [37, 38]. With the emergence of novel immunotherapies, there has been increasing focus on the tumour microenvironment (TME) in UM to better understand the mechanisms of immune evasion. Studies have identified the immune infiltration in UM from bulk tissue data, however, single-cell studies have revealed the complex and heterogeneous nature of the TME in various cancers, highlighting the potential value for this in understanding UM [39, 40].

In this study, we performed a comprehensive characterization of the tumoral immune infiltrate in primary uveal melanoma (UM), integrating single-cell transcriptomic data with multiparametric flow cytometric analysis. Our findings provide novel insights into the cellular heterogeneity and immune landscape of UM tumours and the potential

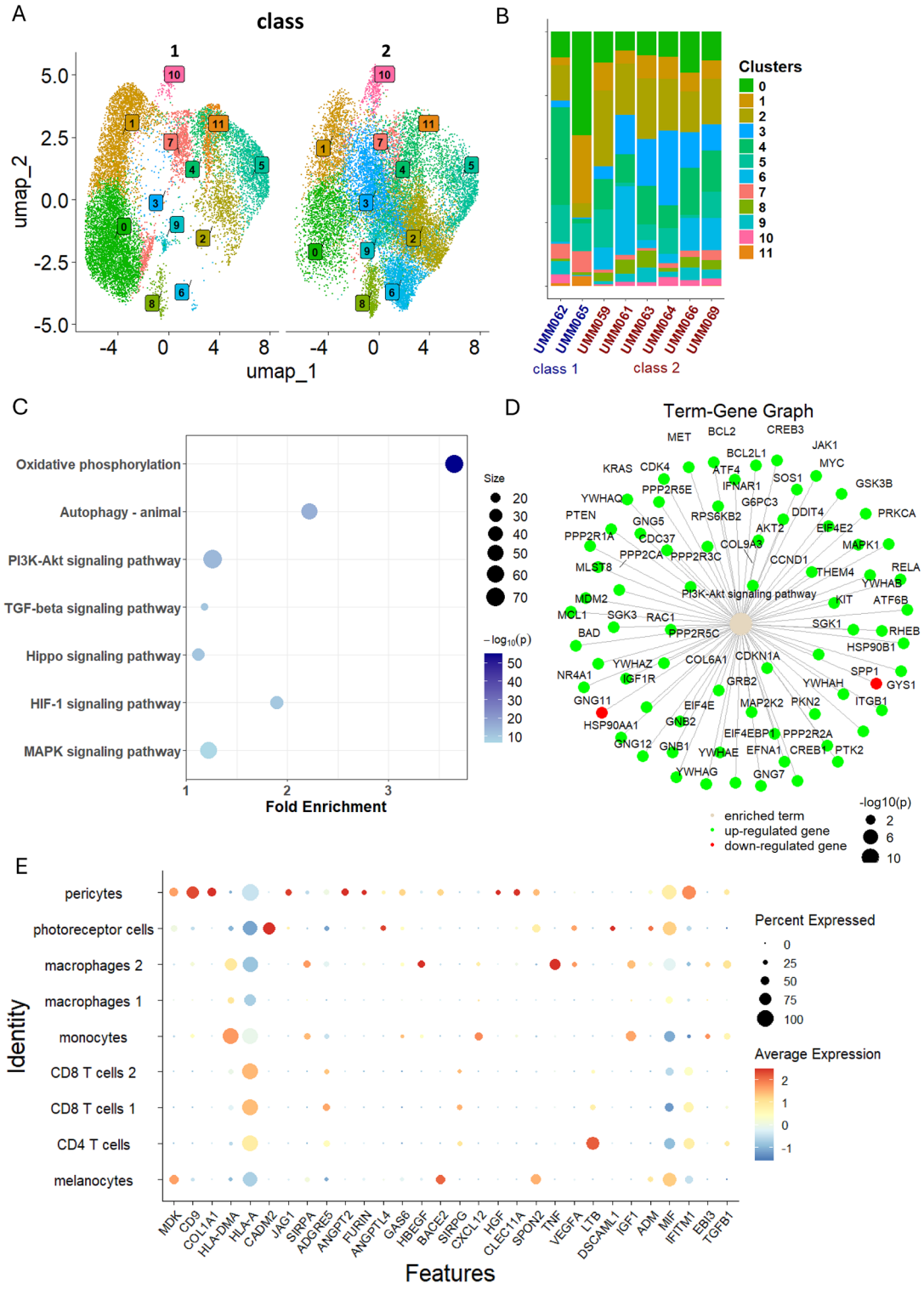

Fig. 2 Pathway enrichment analysis and interactions of cancer cell clusters and infiltrating immune cells. **A** Sub-clustering of UM primary tumour melanocytes. 11 different clusters were identified based on unsupervised clustering. **B** Frequency of melanocyte clusters per patient, cluster 3 and 6 are expanded in class 2 UM compared to class 1. **C** Pathway enrichment analysis of combined clusters 3 and 6 compared to all other melanocyte clusters, dot size represents the number of upregulated genes in the pathway and colour indicates *p* value. **D** Term plot depicting the member genes of the PI3K-AKT signalling pathway that were upregulated (green) or downregulated (red) in the combined cluster 3 and 6 compared to all other melanocyte clusters of UM primary tumour samples. **E** Nichnet analysis depicting receptor ligand interactions between combined cluster 3 and 6 cell (receiver cells) expressed receptors and potential ligands from all other cell subsets (sender cells) at the primary tumour. Percent expressed refers to the percentage of sender cells that express the corresponding ligand.

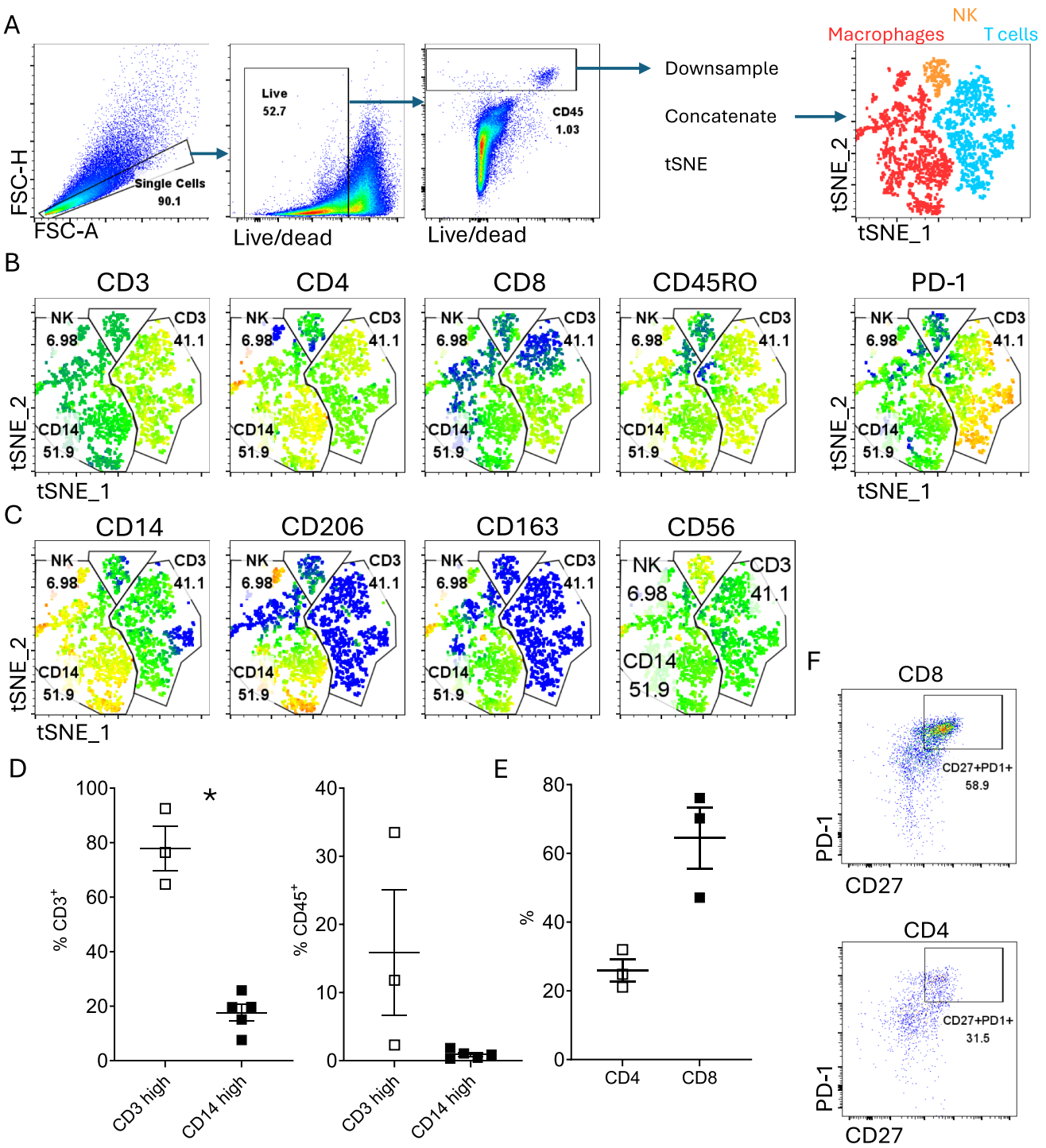

Fig. 3 UM primary tumour infiltrating immune cell flow cytometric analysis. **A** Flow cytometric analysis and dimensionality reduction approach used. Following exclusion of multiplets and dead cells, CD45 cells were selected and downsampled in order to include the same number of events per sample prior to concatenation and dimensionality reduction. 3 major cell types were identified, macrophages, NK and T cells. **B** T and NK cell related marker expression. **C** tSNE plot depicting the expression of macrophage and NK cell related markers across 3 major cell populations. **D** Based on the flow cytometric analysis we identified 2 immune related subtypes of UM, a lymphoid that was rich in infiltrating CD3 + cells (CD3 high) and a myeloid that was rich in CD14 + cells (CD14 high). Percentage of CD3 + cells, as part of the CD45 +, and total CD45 + immune cell infiltrate in CD3 high and CD14 high UM primary tumours. **E** CD4 + and CD8 + T cell distributions in the lymphoid UM tumours. **F** Representative PD-1 and CD27 expression by infiltrating CD4 and CD8 + T cells of the lymphoid UM. Each symbol represents a different sample, mean ± SEM is shown, statistical analysis was performed by two-tailed, non-parametric, paired *t*-test, $*p < 0.05$.

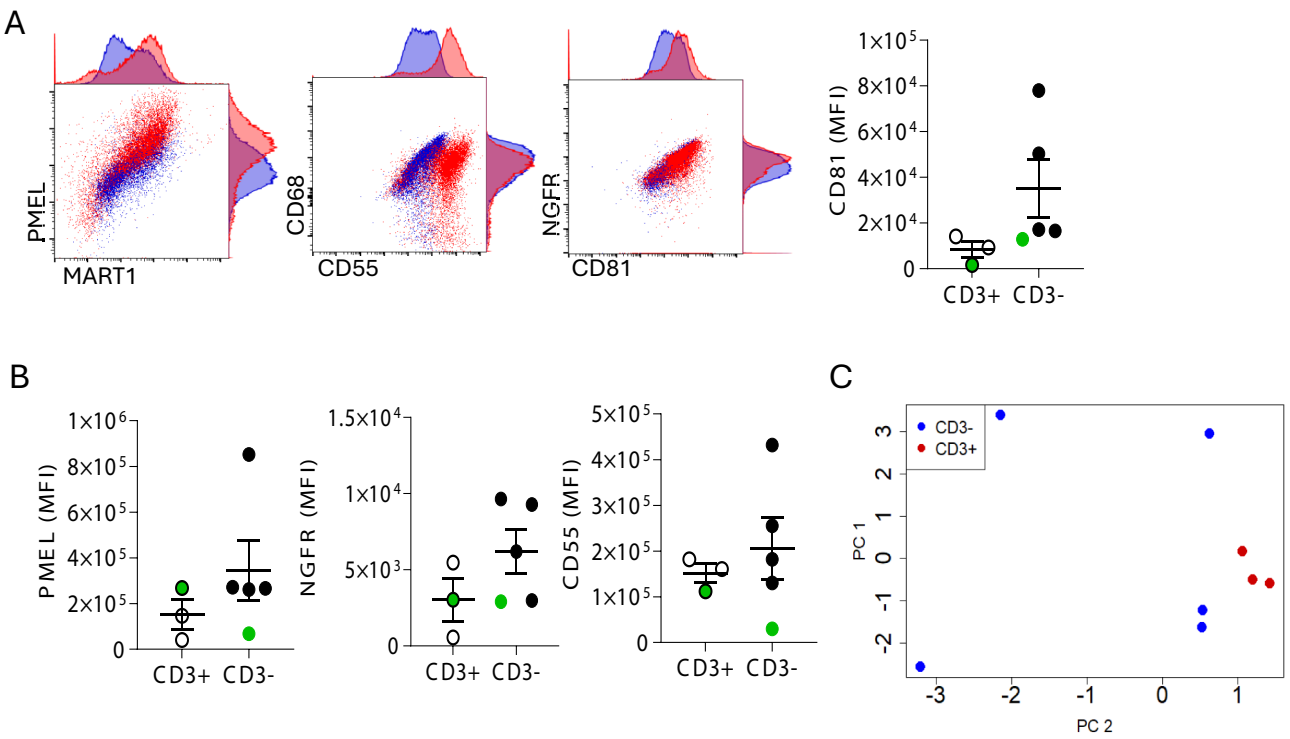

Fig. 4 UM primary tumour stromal cell flow cytometric analysis. **A** Representative flow cytometric analysis of live CD45- primary tumour cells, blue indicates sample with low CD3 T cell infiltration (CD3-) and red sample with high CD3 T cell infiltrate (CD3 +), MFI of stromal CD81 expression is shown. **B** MFI for stromal cell expression of PMEL, NGFR and CD55. Each symbol represents a different sample, mean ± SEM is shown, symbols in green indicate BAP1 negative samples, statistical analysis was performed by two tailed non parametric, *t*-test. **C** Principle component analysis (PCA) of flow cytometry derived expression data. Lymphoid (CD3 +) and non-lymphoid (CD3-) samples are shown.

mechanisms driving tumour progression and immune evasion. This observation aligns with previous studies showing that, in contrast to other solid tumours, the TME in primary UM is associated with poor prognosis [41, 42].

We identified distinct melanocyte subpopulations exclusive to class 2 tumours that exhibit significant copy number variations, particularly on chromosome 8, and are enriched in hypoxia, metabolic, and proliferative signalling pathways. These clusters may represent more aggressive or evolutionarily advanced tumour subtypes, consistent with the profiles of class 2 tumours, potentially contributing to the higher metastatic risk observed in UM with loss of BAP1expression and monosomy 3 [13, 43]. In particular, it has been shown that BAP1 loss can generate an immunosuppressive microenvironment through MERTK (found on macrophages) binding to PROS1 (secreted by tumour cells) promoting M2 macrophage (immune-dampening) polarization and immune evasion [44]. So not only do the class 2 tumours have a more aggressive phenotype, but this also suggests that they have a dual effect, allowing immune evasion.

Receptor–ligand interaction analyses revealed complex crosstalk between tumour cells and the surrounding stromal and immune compartments, with particularly strong interactions involving pericytes and macrophages. These findings suggest that specific tumour–microenvironment interactions may play a pivotal role in shaping tumour behaviour and promoting immune suppression or evasion.

Flow cytometric profiling validated the transcriptional observations and further revealed two distinct immune infiltration patterns among primary tumours. A subset of tumours demonstrated robust T cell infiltration dominated by memory-like $CD8^+$ T cells expressing CD27 and PD-1, indicative of an ongoing yet potentially exhausted antitumour immune response. Conversely, tumours with low T cell infiltration showed enrichment in myeloid cells and elevated expression of markers such as CD81 and NGFR, which have previously been associated with metastatic potential and tumour invasiveness in melanoma. Although immune cell infiltration in most solid tumours is typically associated with effective antitumour responses, this is not the case in UM, suggesting that additional therapeutic support may be necessary to restore effective immune activity [45].

Together, these results emphasize the heterogeneity of UM at the cellular and immunological level and underscore the need for stratified therapeutic strategies that account for the variable immune cell infiltrate observed

herein. Although further characterisation of immune cell infiltration in a larger cohort of patients is needed and would allow for assessment of possible associations between the herein identified two distinct types of primary UM tumours based on TME and previously described prognostic characteristics such as HLA type, PRAME protein expression and AJCC classification in order to assess links between TME and risk of metastasis. The presence of immunologically distinct tumour microenvironments suggests that immunotherapeutic interventions may benefit from patient-specific tailoring. Moreover, our identification of aggressive tumour cell states and their potential interactions with the stromal and immune cells provides a rationale for the development of novel combinatorial therapies targeting both tumour-intrinsic factors and the tumour immune microenvironment.

Future studies should aim to expand on these findings by including metastatic samples and longitudinal analyses, which could further illuminate the dynamic evolution of the immune landscape in UM and its implications for treatment resistance and disease progression.

Supplementary Information The online version contains supplementary material available at https://doi.org/10.1007/s00262-025-04198-7.

Acknowledgements We would like to acknowledge the patients that participated in this study. Without their contribution and support the study wouldn't be possible.

Author contributions KP: Conceptualization, Data curation, Methodology, Validation, Writing – original draft Visualization, SO: Data curation, Writing – original draft, GF: Data curation, Writing – original draft, NH: Data curation, Resources, Writing – original draft, ST: Data curation, Formal analysis, Software, Writing – original draft, SK: Conceptualization, Data curation, Investigation, Resources, Supervision, Project administration, Writing – original draft, AF: Conceptualization, Data curation, Formal analysis, Funding acquisition, Investigation, Methodology, Project administration, Resources, Supervision, Validation, Visualization, Writing – original draft, Writing – review & editing.

Funding AF has received funding from the Health Research Board under grant number HRB-EIA2022-002, DCU and the Hellenic Foundation of Research and Innovation (HFRI) HFRI-24889.

Data availability The data are available upon reasonable request.

Declarations

Competing interests The authors declare no competing interests.

References

1. Mahendraraj K, Lau C, Lee I, Chamberlain R (2016) Trends in incidence, survival, and management of uveal melanoma: a population-based study of 7,516 patients from the Surveillance, Epidemiology, and End Results database (1973–2012). Clin Ophthalmol 10:2113–2119
2. Weis E (2006) The association between host susceptibility factors and uveal melanoma: a meta-analysis. Arch Ophthalmol 124:54
3. Andreoli MT, Mieler WF, Leiderman YI (2015) Epidemiological trends in uveal melanoma. Br J Ophthalmol 99:1550–1553
4. Virgili G et al (2007) Incidence of uveal melanoma in Europe. Ophthalmology 114:2309-2315.e2
5. Baily C et al (2019) Uveal melanoma in Ireland. Ocul Oncol Pathol 5:195–204
6. Kaliki S, Shields CL (2017) Uveal melanoma: relatively rare but deadly cancer. Eye 31:241–257
7. Kujala E, Ma¨kitie T, Kivela¨ T (2003) Very long-term prognosis of patients with malignant uveal melanoma. Invest Ophthalmol Vis Sci 44:4651
8. Garg G et al (2022) Patients presenting with metastases: stage IV uveal melanoma, an international study. Br J Ophthalmol 106:510–517
9. Lorigan JG, Wallace S, Mavligit GM (1991) The prevalence and location of metastases from ocular melanoma: imaging study in 110 patients. Am J Roentgenol 157:1279–1281
10. Decatur CL et al (2016) Driver mutations in uveal melanoma: associations with gene expression profile and patient outcomes. JAMA Ophthalmol 134:728
11. Field MG et al (2018) Punctuated evolution of canonical genomic aberrations in uveal melanoma. Nat Commun 9:116
12. Harbour JW et al (2010) Frequent mutation of *BAP1* in metastasizing uveal melanomas. Science 330:1410–1413
13. Kalirai H, Dodson A, Faqir S, Damato BE, Coupland SE (2014) Lack of BAP1 protein expression in uveal melanoma is associated with increased metastatic risk and has utility in routine prognostic testing. Br J Cancer 111(7):1373–1380. https://doi.org/10.1038/bjc.2014.417
14. Kennedy S et al (2024) Prognostic value of BAP1 protein expression in uveal melanoma. Am J Surg Pathol 48:329–336
15. Kuznetsov JN et al (2019) BAP1 regulates epigenetic switch from pluripotency to differentiation in developmental lineages giving rise to BAP1-mutant cancers. Sci Adv 5:eaax1738
16. Ventii KH et al (2008) *BRCA1*-associated protein-1 is a tumor suppressor that requires deubiquitinating activity and nuclear localization. Cancer Res 68:6953–6962
17. Lee S-A et al (2022) BAP1 promotes the repair of UV-induced DNA damage via PARP1-mediated recruitment to damage sites and control of activity and stability. Cell Death Differ 29:2381–2398
18. Onken MD, Worley LA, Tuscan MD, Harbour JW (2010) An accurate, clinically feasible multi-gene expression assay for predicting metastasis in uveal melanoma. J Mol Diagn 12:461–468
19. Cassoux N et al (2014) Genome-wide profiling is a clinically relevant and affordable prognostic test in posterior uveal melanoma. Br J Ophthalmol 98:769–774

20. Onken MD et al (2012) Collaborative ocular oncology group report number 1: prospective validation of a multi-gene prognostic assay in uveal melanoma. Ophthalmology 119:1596–1603
21. Robertson AG et al (2017) Integrative analysis identifies four molecular and clinical subsets in uveal melanoma. Cancer Cell 32:204-220.e15
22. Beasley AB, Preen DB, McLenachan S, Gray ES, Chen FK (2023) Incidence and mortality of uveal melanoma in Australia (1982–2014). Br J Ophthalmol 107:406–411
23. Singh AD, Turell ME, Topham AK (2011) Uveal melanoma: trends in incidence, treatment, and survival. Ophthalmology 118:1881–1885
24. Gill V et al (2022) Trends in uveal melanoma presentation and survival during five decades: a nationwide survey of 3898 Swedish patients. Front Med 9:926034
25. Rantala ES, Hernberg MM, Piperno-Neumann S, Grossniklaus HE, Kivelä TT (2022) Metastatic uveal melanoma: the final frontier. Prog Retin Eye Res 90:101041
26. Carvajal RD et al (2018) Selumetinib in combination with dacarbazine in patients with metastatic uveal melanoma: a phase III, multicenter, randomized trial (SUMIT). J Clin Oncol 36:1232–1239
27. Luke JJ et al (2020) Randomized phase II trial and tumor mutational spectrum analysis from cabozantinib versus chemotherapy in metastatic uveal melanoma (Alliance A091201). Clin Cancer Res 26:804–811
28. Algazi AP et al (2016) Clinical outcomes in metastatic uveal melanoma treated with PD-1 and PD-L1 antibodies. Cancer 122:3344–3353
29. Zimmer L et al (2015) Phase II decog-study of Ipilimumab in pretreated and treatment-naïve patients with metastatic uveal melanoma. PLoS ONE 10:e0118564
30. Hassel JC et al (2023) Three-year overall survival with Tebentafusp in metastatic uveal melanoma. N Engl J Med 389:2256–2266
31. participants in the 1st Human Cell Atlas Jamboree *et al.* EmptyDrops: distinguishing cells from empty droplets in droplet-based single-cell RNA sequencing data. *Genome Biol.* **20**, 63 (2019).
32. Hao Y et al (2024) Dictionary learning for integrative, multimodal and scalable single-cell analysis. Nat Biotechnol 42:293–304
33. McGinnis CS, Murrow LM, Gartner ZJ (2019) Doubletfinder: doublet detection in single-cell rna sequencing data using artificial nearest neighbors. Cell Syst 8:329-337.e4
34. Hafemeister C, Satija R (2019) Normalization and variance stabilization of single-cell RNA-seq data using regularized negative binomial regression. Genome Biol 20:296
35. Sisley K et al (2000) Association of specific chromosome alterations with tumour phenotype in posterior uveal melanoma. Br J Cancer 82:330–338
36. Basile MS et al (2019) Immunobiology of uveal melanoma: state of the art and therapeutic targets. Front Oncol 9:1145
37. Oliva M, Rullan AJ, Piulats JM (2016) Uveal melanoma as a target for immune-therapy. Ann Transl Med 4:172
38. Matsuo H, Kamatani T, Hamba Y, Boroevich KA, Tsunoda T (2022) Association between high immune activity and worse prognosis in uveal melanoma and low-grade glioma in TCGA transcriptomic data. BMC Genomics 23:351
39. Triozzi PL et al (2019) Molecular profiling of primary uveal melanomas with tumor-infiltrating lymphocytes. Oncoimmunology 8:e947169
40. Bronkhorst IHG, Jager MJ (2012) Uveal melanoma: the inflammatory microenvironment. J Innate Immun 4:454–462
41. Edge SB, Compton CC (2010) The American joint committee on cancer: the 7th edition of the AJCC cancer staging manual and the future of TNM. Ann Surg Oncol 17:1471–1474
42. Mazloumi M et al (2020) Accuracy of the cancer genome atlas classification vs american joint committee on cancer classification for prediction of metastasis in patients with Uveal Melanoma. JAMA Ophthalmol 138:260–267
43. Nathan P et al (2021) Overall survival benefit with tebentafusp in metastatic uveal melanoma. N Engl J Med 385:1196–1206
44. Lv X, Ding M, Liu Y (2022) Landscape of infiltrated immune cell characterization in uveal melanoma to improve immune checkpoint blockade therapy. Front Immunol 13:848455
45. Basile MS et al (2019) Differential modulation and prognostic values of immune-escape genes in uveal melanoma. PLoS ONE 14:e0210276